

ARTICLE

Received 24 May 2014 | Accepted 8 Jul 2014 | Published 18 Aug 2014

DOI: 10.1038/ncomms5628

Switching between humoral and cellular immune responses in *Drosophila* is guided by the cytokine GBP

Seiji Tsuzuki^{1,*}, Hitoshi Matsumoto^{1,*}, Shunsuke Furihata¹, Masasuke Ryuda¹, Hirotohi Tanaka¹, Eui Jae Sung², Gary S. Bird^{2,3}, Yixing Zhou², Stephen B. Shears² & Yoichi Hayakawa¹

Insects combat infection through carefully measured cellular (for example, phagocytosis) and humoral (for example, secretion of antimicrobial peptides (AMPs)) innate immune responses. Little is known concerning how these different defense mechanisms are coordinated. Here, we use insect plasmatocytes and hemocyte-like *Drosophila* S2 cells to characterize mechanisms of immunity that operate in the haemocoel. We demonstrate that a *Drosophila* cytokine, growth-blocking peptides (GBP), acts through the phospholipase C (PLC)/Ca²⁺ signalling cascade to mediate the secretion of Pvf, a ligand for platelet-derived growth factor- and vascular endothelial growth factor-receptor (Pvr) homologue. Activated Pvr recruits extracellular signal-regulated protein kinase to inhibit humoral immune responses, while stimulating cell 'spreading', an initiating event in cellular immunity. The double-stranded RNA (dsRNA)-targeted knockdown of either *Pvf2* or *Pvr* inhibits GBP-mediated cell spreading and activates AMP expression. Conversely, *Pvf2* overexpression enhances cell spreading but inhibits AMP expression. Thus, we describe mechanisms to initiate immune programs that are either humoral or cellular in nature, but not both; such immunophysiological polarization may minimize homeostatic imbalance during infection.

¹Department of Applied Biological Sciences, Saga University, Saga 840-8502, Japan. ²Inositol Signaling Section, NIEHS, NIH, DHHS, Research Triangle Park, North Carolina 27709, USA. ³Calcium Regulation Section, NIEHS, NIH, DHHS, Research Triangle Park, North Carolina 27709, USA. * These authors contributed equally to this work. Correspondence and requests for materials should be addressed to Y.H. (email: hayakayo@cc.saga-u.ac.jp).

Many components of innate immunity share an ancient origin in metazoan evolution, and so *Drosophila* has long been considered as a relevant and genetically tractable model for studying general mechanisms of innate immunity in animals¹. For example, in *Drosophila* larvae, the major blood immunoreactive cells that defend the haemocoel against its invasion by foreign organisms are plasmatocytes^{1–3}, which normally comprise 90–95% of all mature hemocytes^{4–6}. Plasmatocytes, which exhibit both cellular and humoral immune activities, are considered to be equivalent to mammalian cells of the monocyte/macrophage lineage⁷. The main cellular responses of plasmatocytes are phagocytosis and encapsulation; humoral responses involve the synthesis and secretion of antimicrobial peptides (AMPs). More recent studies have revealed that changes in innate immune activities can also combat non-infectious stresses and participate in maintenance of organismic homeostasis^{8,9}. Ideally, there should be minimal disturbance of these homeostatic functions, and thus protection from collateral tissue damage, when immune cells are mobilized against invading pathogens^{9,10}. Thus the processes of immunity and inflammation are anticipated to involve careful coordination and intricate cross-talk between multiple stimulatory as well as inhibitory signalling pathways, but the mechanisms are poorly understood.

In a variety of insect species, cytokine-mediated activation of plasmatocyte cell spreading is a prelude to these cells becoming competent to perform phagocytosis and encapsulation (that is, the process of cellular immunity)^{2,11}. Many of these cytokines, which have variously been described as either growth-blocking peptides ('GBPs')⁸, or plasmatocyte-spreading peptides^{8,12–14}, are activated on their release from the C terminus of larger propeptides by serine protease activity. These bioactive peptides contain a consensus motif: Cx₂Gx_(4–6)Gx_(1–2)C[K/R]¹³. The active form of *Drosophila* GBP contains 24 amino-acid residues; overexpression of GBP in *Drosophila* larvae increases the expression of antimicrobial peptide (AMP) genes such as *Metchnikowin* (*Mtk*) and *Diptericin* (*Dpt*), which are markers for humoral aspects of innate immunity⁸. In *Drosophila*, GBP also regulates immune responses to non-infectious environmental challenges such as physical stress or exposure to temperature changes⁸. The current study investigates both positive and negative cell-signalling control over immune responses to *Drosophila* GBP. However, plasmatocytes are not an ideal model system for studying immune responses, because their isolation is a tedious procedure, which yields only limited quantities of cells. Thus, another goal in our study is to develop a more tractable cell model to study GBP-dependent immunological mechanisms. Previous work has shown that *Drosophila* S2 cells recapitulate key elements of the innate immune program^{15–17}. S2 cells are derived from embryonic hemocyte lineages, and they are able to phagocytose microbes and secrete AMP⁷.

The experiments described in this study lead us to uncover a linear pathway by which GBP is as an upstream activator of the platelet-derived growth factor- and vascular endothelial growth factor-receptor homologue (*Pvr*). The latter finding was initially unexpected as previous work has indicated that *Pvr* enforces an inhibitory pathway in humoral innate immunity¹⁸. Indeed, in the current study, we confirm that activation of *Pvr* downstream of GBP restrains expression of AMPs in both plasmatocytes and S2 cells. However, we also demonstrate that the *Pvr* cascade activates cellular aspects of the innate immune pathway. That is, the innate immune functionality of plasmatocytes *per se* is not inhibited by *Pvr*, but rather, the nature of their immune response is reprogrammed. In this way, we demonstrate that individual cells respond to the different roles of GBP by becoming polarized to exhibit either the humoral or cellular arm of the innate immune process.

Results

Cell spreading in *Pseudaletia separata* and *Drosophila* plasmatocytes.

Cytokine-induced cell spreading offers a phenotypic readout of the first step in the activation of the cellular arm of the innate immune pathway. Plasmatocyte spreading is characterized by an increased adhesion to foreign surfaces and a change from a spherical shape into a more flattened and extended morphology that can be readily quantified^{12,14}. *P. separata* GBP (PsGBP)^{19–21} and *Drosophila* GBP⁸ induced these morphological changes in plasmatocytes isolated from larvae of the armyworm *P. separata* (Fig. 1a) and *Drosophila* (Fig. 1b), respectively. As in previous studies, we employed the active version of these peptides that are released following serine protease action on the inactive propeptide precursors^{8,13}.

Previous work has shown that extracellular Ca²⁺ is required in order that hemocyte spreading can be induced by plasmatocyte-spreading peptides from *Spodoptera exigua*²². Likewise, we also found that PsGBP-dependent spreading of *P. separata* plasmatocytes was inhibited when extracellular Ca²⁺ was chelated with either EDTA or EGTA (Fig. 1c). Recently, we demonstrated that extracellular Ca²⁺ is also required for maximizing the intracellular Ca²⁺ signal that GBP elicits from *Drosophila* S3 cells on its activation of PLC²³. We therefore investigated if this signalling response might participate in plasmatocyte spreading. Inhibition of PLC in *P. separata* plasmatocytes by addition of U73122 prevented PsGBP from inducing cell spreading (Fig. 1c). Furthermore, we also made the novel observation that PsGBP-dependent activation of plasmatocytes was attenuated by (p-amidinophenyl) methylsulphonyl fluoride (APMSF), a serine protease inhibitor (Fig. 1c). Since active PsGBP was used in these assays, the inhibition by APMSF suggested that the processing of a different precursor protein might be involved in PsGBP-induced spreading of plasmatocytes.

Cellular activation of S2 cells by GBP. The isolation of plasmatocytes from *Drosophila* larvae is a tedious procedure that yields relatively few cells. One of the goals of our study was to develop a more tractable cell model system in which to study the GBP-dependent signalling mechanisms that promote plasmatocyte spreading in *Drosophila*^{16,17}. It is known that S2 cells are likely derived from embryonic hemocyte lineages⁷. In addition, we have noted that S2 cells incubated for extended periods in a microplate slowly develop a plasmatocyte-like 'spreading' phenotype and also encapsulate foreign objects such as dextran beads (Supplementary Fig. 1a,b). We have now made the notable observation that *Drosophila* GBP significantly accelerated the acquisition of the spreading phenotype in a concentration-dependent manner (Fig. 1d, Supplementary Fig. 1b). These observations led us to use S2 cells as a model for characterizing the GBP-induced signalling events that promote cell spreading.

Extracellular signal-regulated protein kinase activation by GBP.

In earlier work with the MaBr4 fat body cell line from Lepidoptera *Mamesta brassicae*, we found that *M. brassicae* GBP activates the extracellular signal-regulated protein kinase (ERK)²⁴. Western blotting revealed that GBP stimulated phosphorylation of *Drosophila* ERK (the gene product of *rolled*) in S2 cells (Fig. 1e). We next found that GBP-induced ERK activation was blocked by the addition of either a PLC inhibitor (U73122) or an inositol triphosphate (IP₃) receptor (*Itpr*) antagonist (TMB-8) (Fig. 1f). These data indicate that ERK lies downstream of PLC activation. We confirmed that *Drosophila* GBP activated PLC in S2 cells by high-performance liquid chromatography (HPLC) analysis of inositol phosphate levels in control and GBP-

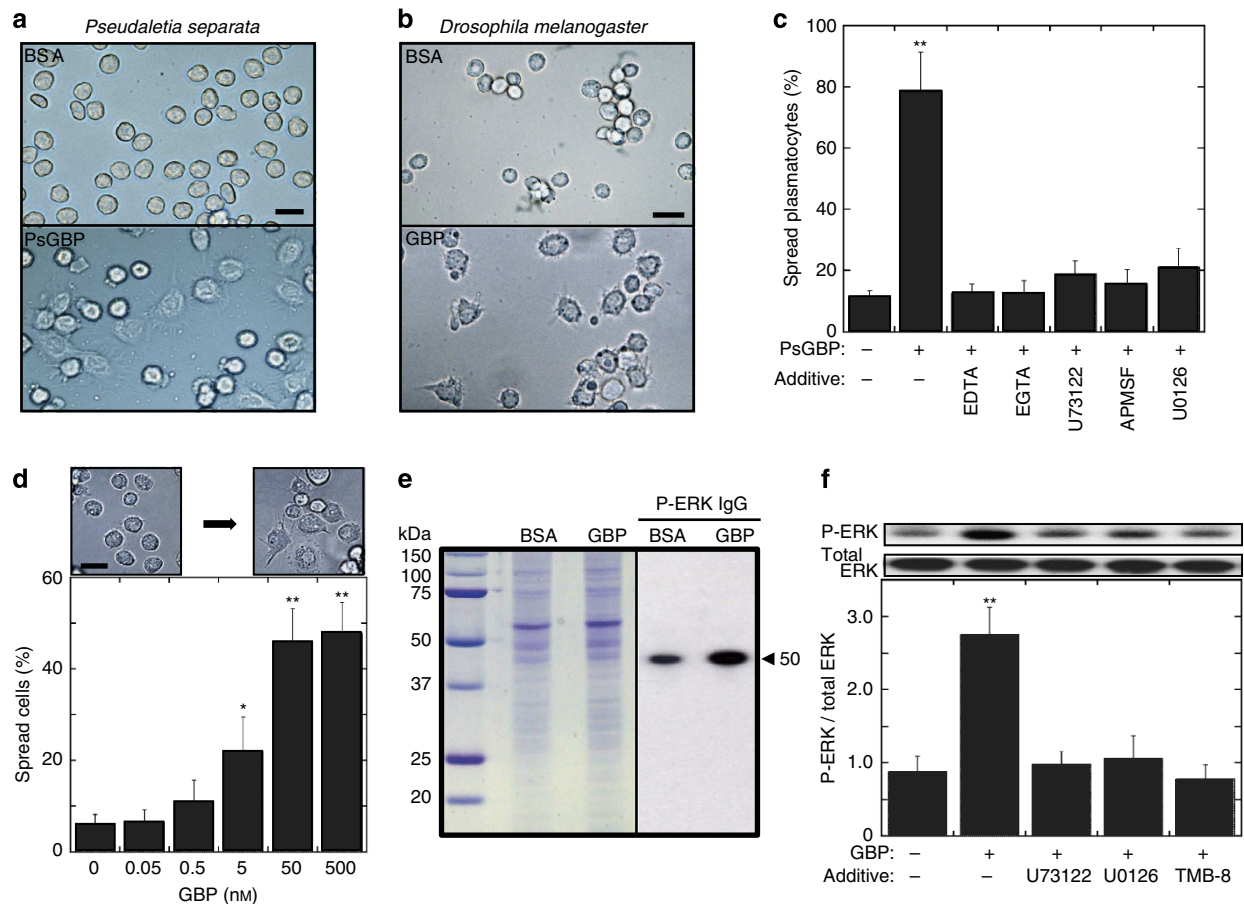


Figure 1 | Spreading response of plasmatocytes and *Drosophila* S2 cells. (a) Representative images of *P. separate* larval plasmatocytes incubated with either 20 nM PsGBP (lower) or BSA (upper) for 30 min. Scale bar, 25 μ m. (b) Representative images of *Drosophila* larval plasmatocytes incubated with either 20 nM GBP (lower) or BSA (upper) for 20 min. Scale bar, 20 μ m. (c) Quantification of PsGBP-mediated spreading activity of *P. separate* larval plasmatocytes. Where indicated, either 10 mM EDTA, 10 mM EGTA, 10 μ M U73122, 100 μ M APMSF or 10 μ M U0126 was added 5 min before 20 nM PsGBP. Each bar represents the mean \pm s.d. for eight independent determinations. ** $P < 0.01$: Significant differences from control (- GBP/- Additive) value are indicated by Tukey's HSD. (d) Representative images (upper) of 50 nM GBP-induced spreading of S2 cells and quantification of cell spreading (lower) 30 min after addition of the indicated concentration of GBP. Each value represents the mean \pm s.d. for six independent determinations * $P < 0.05$; ** $P < 0.01$: Significant differences from control (0 nM GBP) value are indicated by Tukey's HSD. (e) Western blots of GBP-induced phosphorylation of ERK in S2 cells. Coomassie Brilliant Blue stained SDS/PAGE gel (left), and immunoblotting with phosphorylated ERK IgG (right). The arrowhead indicates the ERK band. (f) The inhibition of GBP-induced ERK activation. Where indicated, either 10 μ M U73122, 10 μ M U0126, or 10 μ M TMB-8 was added 10 min before 20 nM GBP and ERK was assayed after 3 min-incubation with GBP. Each bar represents the mean \pm s.d. for four independent determinations. ** $P < 0.01$: Significantly different from control (- GBP/- Additive) value. Full blot is supplied in Supplementary Fig. 10.

stimulated S2 cells (Fig. 2a). We further found that GBP elevated levels of 1,4,5 IP₃ and 1,4,5,6 IP₄ 4-5 fold (Fig. 2b). The former promotes calcium mobilization²⁵, and the latter is a transcriptional regulator²⁶.

We demonstrated that GBP significantly elevated intracellular Ca²⁺ concentrations in S2 cells in a concentration-dependent manner (Supplementary Fig. 2a,b). The GBP-induced elevation of Ca²⁺ concentration was significantly repressed by the chelation of extracellular Ca²⁺ by the addition of either EDTA, EGTA or BAPTA or by inhibition of PLC by U73122 (Fig. 2c). We furthermore confirmed the contribution of the PLC/IP₃ cascade by showing that GBP-dependent Ca²⁺ elevation was inhibited by dsRNA-mediated knockdown of *Itpr* expression in S2 cells (Fig. 2d) as well as the *Itpr* antagonist (TMB-8) (Fig. 2c).

Chelation of extracellular Ca²⁺ by the addition of EDTA, EGTA or BAPTA substantially reduced GBP-induced activation of ERK (Fig. 2e). Moreover, cell treatment with dsRNA against *Itpr* also repressed GBP-dependent ERK activation (Fig. 2f) and cell spreading in S2 cells (Supplementary Fig. 3). Thus, PLC

activation by GBP has immunophysiological consequences. Furthermore, we found that the MEK inhibitor U0126 did not affect GBP-induced elevation of intracellular Ca²⁺ (Fig. 2c), consistent with ERK activation lying downstream of intracellular Ca²⁺ elevation. There are several intracellular signalling pathways that directly couple Ca²⁺ mobilization to ERK activation^{27,28}. However, this does not seem to be the case in our experiments, because the stimulation of ERK phosphorylation by GBP was inhibited by the serine protease inhibitor APMSF (Fig. 2e). Since APMSF did not affect the ability of GBP to mobilize Ca²⁺ (Fig. 2c), and in any case the bioactive form of GBP was used, these results indicate that GBP-mediated activation of ERK involves protease-dependent signalling events that are downstream of Ca²⁺ mobilization. Therefore, we next sought further information concerning the mechanisms that are involved.

GBP-induced signalling events lead to Pvr activation. Previous reports have shown that ERK can be activated by the Pvf/Pvr

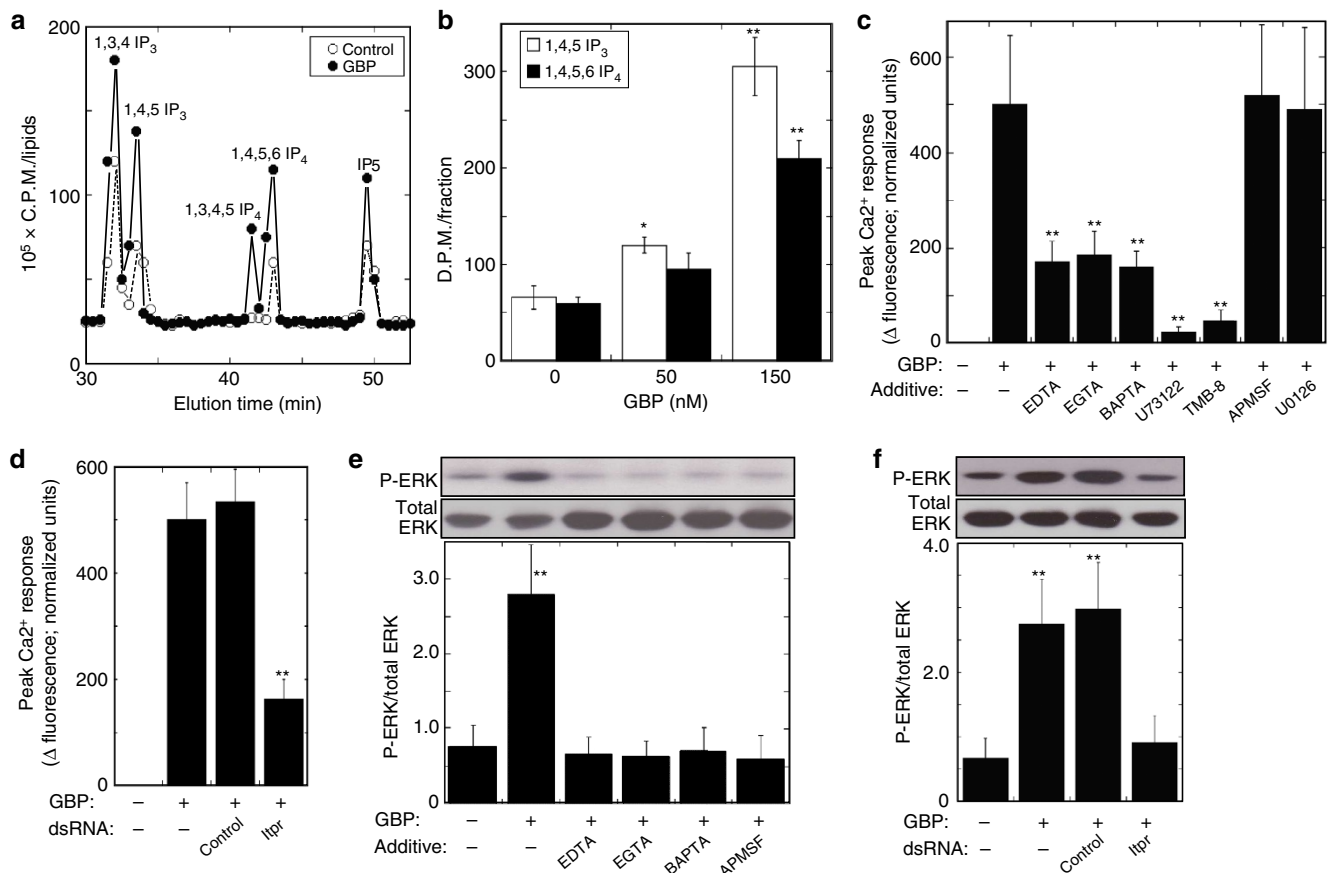


Figure 2 | Characterization of GBP-dependent signalling in *Drosophila* S2 cells. (a) Q-100 SAX HPLC analysis of the [³H]-labelled inositol phosphates in S2 cells treated with either 50 nM GBP or vehicle for 45 min. [³H]-labelled inositol phosphates were analysed using a 4.6 × 250 mm Q-100 HPLC column (Thomson Instruments, USA) with an in-line detector. **(b)** Effects of GBP on the level of 1,4,5 IP₃ and 1,4,5,6 IP₄. Each value represents the mean ± s.d. for three independent determinations **P* < 0.05; ***P* < 0.01: Significant differences from control (0 nM GBP) value are indicated by Tukey's HSD. **(c)** Characterization of the nature of GBP-induced intracellular Ca²⁺ elevation in GCaMP3-expressing S2 cells. Where indicated, either 10 mM EDTA, 10 mM EGTA, 10 mM BAPTA, 10 μM U73122, 10 μM TMB-8, 100 μM APMSF or 10 μM U0126 was added 10 min before 20 nM GBP. Peak Ca²⁺-dependent fluorescence signals were normalized to control (+ GBP/-Additive) values to indicate relative maximum Ca²⁺ signals. Each value represents the mean ± s.d. for three independent determinations. ***P* < 0.01: Significant differences from control (+ GBP/-Additive) value are indicated by Tukey's HSD. **(d)** The inhibition of GBP-induced intracellular Ca²⁺ elevation in GCaMP3-expressing S2 cells by dsRNA targeting of *Itpr*. A 500 bp irrelevant dsRNA from the MEGAscriptTM dsRNA Kit (Life Technologies, USA) served as a negative control. ***P* < 0.01: Significant difference from control (+ GBP/-dsRNA) value is indicated by Tukey's HSD. Other explanations are as in (c). **(e)** Effects on 3 min of GBP-induced activation of ERK in S2 cells when either calcium chelators (10 mM EDTA, 10 mM EGTA, 10 mM BAPTA) or serine protease inhibitor (100 μM APMSF) was added 10 min before 20 nM GBP. Each value represents the mean ± s.d. for five independent determinations. ***P* < 0.01: Significant difference from control (- GBP/-Additive) value is indicated by Tukey's HSD. Full blot was supplied in Supplementary Fig. 10. **(f)** Effects of dsRNA targeting of *Itpr* on GBP-dependent activation of ERK. ***P* < 0.01: Significant differences from control (- GBP/-dsRNA) value are indicated by Tukey's HSD. Other explanations are as in d. Full blot is supplied in Supplementary Fig. 10.

signalling pathway in hemocytes of *Drosophila* larvae and embryos^{29,30}. Furthermore, Pvr ligands (Pvfs) and Pvr have been reported to act upstream of Ras/MAPK in S2 cells³¹. However, it has not previously been considered that GBP might activate Pvf/Pvr signalling; therefore, we next examined that very possibility. The *Drosophila* genome encodes three forms of Pvf (types 1, 2 and 3)²⁹. Real-time PCR (RT-PCR) analysis showed that *Pvf2* is expressed at much higher levels than *Pvf1* and *Pvf3* in S2 cells (Supplementary Fig. 4a). We further found that knockdown of *Pvf2* expression by RNA interference (RNAi) reduced GBP-induced activation of ERK (Fig. 3a). RNAi knockdown of *Pvr* also abolished GBP-dependent ERK activation (Fig. 3a). In contrast, knockdown of either *Pvf1* or *Pvf3* expression had no effects on ERK activation (Fig. 3a; Supplementary Fig. 4b). These data reinforce the particular importance of Pvf2, although they do not exclude a redundant role for Pvf1 and Pvf3, for example in

forming heterodimers with Pvf2. Furthermore, we took the conditioned medium that had been used to culture S2 cells in which *Pvf2* was overexpressed (see Supplementary Fig. 5), and added that to naive S2 cells; that procedure activated ERK while the activation was neutralized when the conditioned medium was preincubated with anti-Pvf2 IgG (Fig. 3b). These data not only indicate that Pvf2 was present in the conditioned medium, but also demonstrate that the Pvf2 was biologically active. By western blot analysis, we also demonstrated that Pvf2 concentrations were increased in culture medium of S2 cells following either the addition of GBP, or the addition of the Ca²⁺ ionophore, A23187 (Fig. 3c). Liquid chromatography mass spectrometry analysis of the immunoreactive band confirmed the presence of Pvf2 (Supplementary Fig. 6). Further evidence of the role of Ca²⁺ was obtained by showing that the release of Pvf2 by GBP was inhibited when Ca²⁺ mobilization was inhibited on the chelation

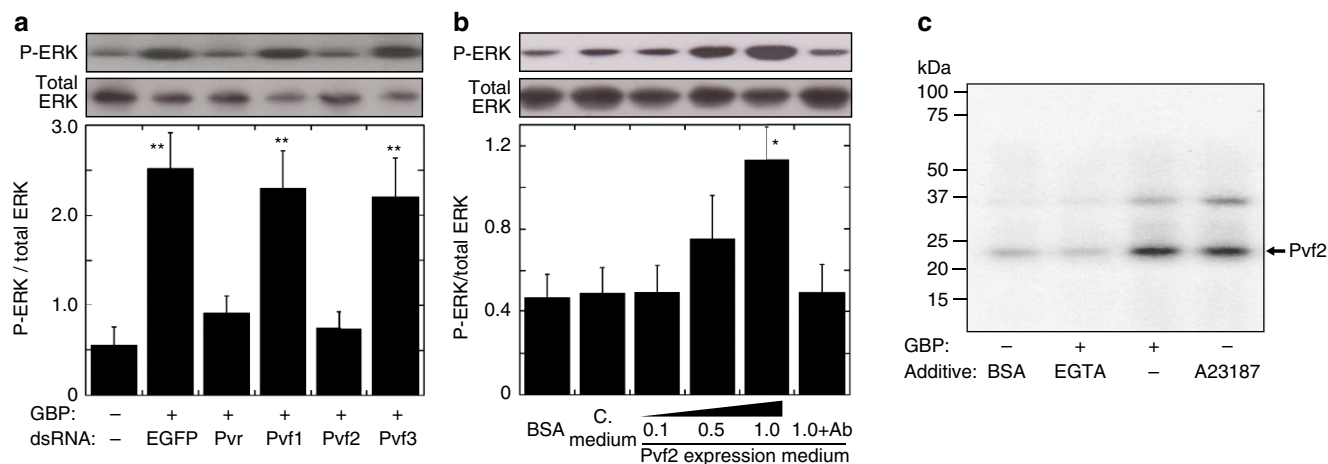


Figure 3 | Analysis of the Pvf/Pvr and ERK mediated cell spreading response in *Drosophila* S2 cells. (a) Effects of dsRNA targeting of either *Pvr* or *Pvf* 1-3 genes on GBP-dependent ERK activation in S2 cells. S2 cells were used three days after adding dsRNA of each target gene as described in the Methods. Where indicated, 20 nM GBP was added for 3 min. Each value represents the mean \pm s.d. for four independent determinations. $**P < 0.01$: Significant differences from control (-GBP/-dsRNA) value are indicated by Tukey's HSD. Full blot was supplied in Supplementary Fig. 11. (b) ERK activation by conditioned medium of *Pvf2*-over-expressing S2 cells. 0.1, 0.5, 1.0: 10-fold diluted, 2-fold diluted and undiluted conditioned media of S2 cell culture (5×10^6 cells per well) were respectively used. C. medium: medium from cultures of control S2 cells. 1.0 + Ab: undiluted conditioned medium preincubated with anti-Pvf2 antibody for 2 h. Each value represents the mean \pm s.d. for five independent determinations. $*P < 0.05$: Significant difference from control (BSA) value is indicated by Tukey's HSD. Full blot is supplied in Supplementary Fig. 11. (c) Western blot of Pvf2 protein in incubation medium of S2 cells stimulated by either 20 nM GBP or 100 nM A23187 for 3 min. In the case of EGTA treatment, S2 cells were preincubated with 10 mM EGTA for 10 min before addition of 20 nM GBP. Liquid chromatography mass spectrometry analysis of the immunoreactive band indicated by the arrow (in GBP-treated sample) showed that two determined peptide fragment sequences  (VPRPEVVHITR and PRPEVVHITR) were found to be completely identical in Pvf2 amino-acid sequence, indicating that this band is Pvf2 precursor protein (see Supplementary Fig. 6).

of extracellular Ca^{2+} by EGTA (Fig. 3c). In conclusion, we have demonstrated that GBP-mediated activation of ERK is dependent on Ca^{2+} -dependent Pvf2 secretion into the culture medium, and the presence of the Pvr.

Immunophysiological role of the Pvr-ERK signalling pathway.

We next found that the MEK inhibitor, U0126, significantly repressed activation of ERK, both in S2 cells treated with GBP (Fig. 1f), and in PsGBP-treated plasmatocytes prepared from the armyworm larvae (Fig. 1c). Furthermore, U0126 inhibited PsGBP-induced spreading of *P. separata* plasmatocytes (Supplementary Fig. 7). These results together with the above observation that RNAi knockdown of *Itpr* repressed GBP-induced spreading as well as ERK activation in S2 cells (Fig. 2f; Supplementary Fig. 3) indicate the importance of ERK activation for cell spreading. Moreover, dsRNA targeting of either *ERK*, *Pvr* or *Pvf2* significantly repressed the GBP-induced spreading in S2 cells (Fig. 4a-c).

As mentioned above, cell spreading offers a phenotypic readout of the first step in the activation of the cellular arm of the innate immune pathway. Thus, our data demonstrated that GBP promotes cellular immune responses through the activation of the Pvf/Pvr-ERK signalling pathway. We reinforced this idea by demonstrating that plasmatocytes prepared from *Drosophila* larvae treated with *Pvr* dsRNA were significantly impaired in their capacity to acquire spread morphology on addition of GBP (Fig. 4d). That conclusion may at first sight appear to be inconsistent with previous report characterizing the Pvr pathway as inhibiting innate immunity¹⁸. However, the latter conclusion is based on the earlier demonstration that the Pvr cascade inhibits AMP synthesis¹⁸—a humoral response—whereas our experiments show that a separate, cellular arm of the innate immune program is activated. We therefore sought to clarify the effects of Pvr expression on the relationship between GBP-induced humoral

and cellular immune responses using transgenic *Drosophila* larvae. We examined expression of *Mtk* in the hemocytes of *Drosophila* larvae in which GBP was overexpressed. In agreement with an earlier study⁸, we found that GBP slightly but significantly increased *Mtk* expression, but to a level that was about 10-fold below that seen in larvae after introducing *S. marcescens* in an acute model of septic injury (Fig. 4e). Moreover, an important new observation in the current study is that the GBP-induced *Mtk* expression level was enhanced almost fivefold in *Pvr* knockdown larvae (Fig. 4e; controls validating the expected changes in GBP and *Pvr* expression are shown in Supplementary Fig. 8). These data show that, in non-infected control larvae, it is the Pvf/Pvr signalling cascade that prevents GBP from maximally stimulating *Mtk* expression. Thus, when *Pvr* expression was knocked down, the GBP-mediated *Mtk* expression attained a level that was only 40% less than that observed in the septic injury model (Fig. 4e).

We further showed that the GBP-dependent *Mtk* and *Dpt* expression levels were significantly enhanced in S2 cells treated with *Pvf2* dsRNA compared with those in control S2 cells (Fig. 5a,b). That is, our data indicate that Pvf2 inhibits this humoral arm of the GBP-induced immune responses. We next examined the effects on cellular and humoral immune responses when *Pvf2* was overexpressed under the control of the Cu^{2+} -inducible metallothionein promoter (Supplementary Fig. 5). We found that *Pvf2* overexpression enhanced spreading of S2 cells irrespective of the presence of GBP (Fig. 5c). On the other hand, GBP-induced *Mtk* and *Dpt* expression levels were significantly repressed by overexpression of *Pvf2* compared with control S2 cells (Fig. 5d,e). In conclusion, our data indicate that the Pvf2/Pvr signalling cascade polarizes the nature of the immune responses of S2 cells and plasmatocytes in favour of mediating the cellular arm of the innate immune pathway.

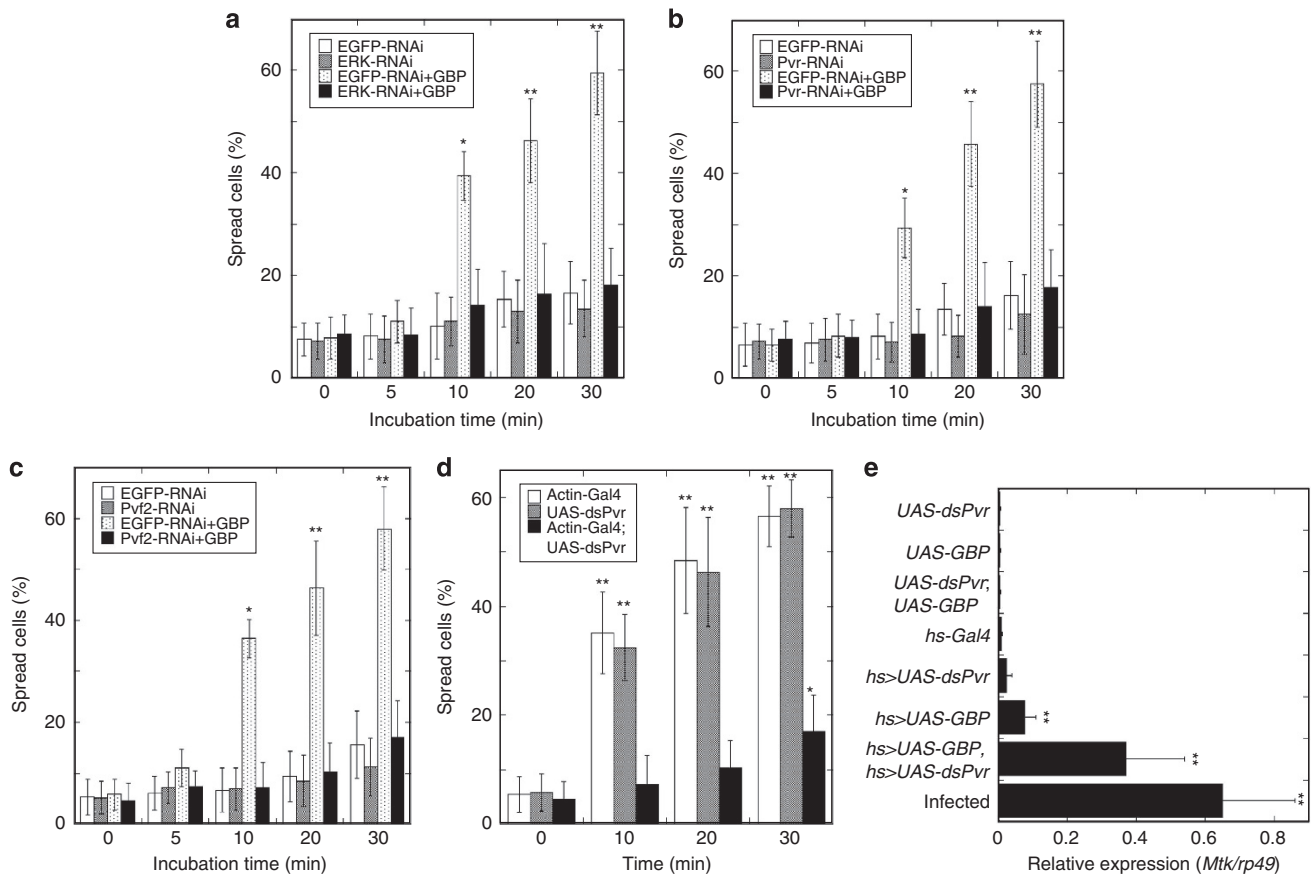


Figure 4 | Effects of altered expression of Pvf/Pvr-ERK signalling related genes on cell spreading and *Metchnikowin* expression. (a–c) Effect of dsRNA targeting of *Erk* (a), *Pvr* (b), or *Pvf2* (c) on spreading of *Drosophila* S2 cells stimulated by 50 nM GBP for the indicated times. Each value represents the mean \pm s.d. for 3–7 independent determinations. * $P < 0.05$; ** $P < 0.01$: Significant differences from control (0 min, EGFP-RNAi) value are indicated by Tukey's HSD. (d) Effect of dsRNA targeting of *Pvr* on GBP-induced spreading of plasmatocytes of *Drosophila* larvae. Plasmatocytes prepared from test larvae were incubated with 20 nM GBP (see Materials and Methods). Average rates of spread plasmatocytes prepared from any test larvae were less than 20% when they were incubated with 20 nM BSA for 30 min. Each value represents the mean \pm s.d. for six independent determinations. * $P < 0.05$; ** $P < 0.01$: Significant differences from control (0 min, Actin-Gal4) value are indicated by Tukey's HSD. (e) Analysis of hemocyte *Mtk* expression with *Pvr* knockdown backgrounds under forced expression of *GBP* in *Drosophila* larvae by quantitative real-time PCR. The *hs-Gal4*-dependent knockdown of *Pvr* and overexpression of *GBP* were induced by heat treatment at 35 °C for 30 min twice with 12 h-interval. Infection was induced by stabbing third instar larvae with a thin tungsten needle previously dipped into a concentrated culture of *Serratia marcescens* 3 h before measuring *Mtk* expression. Induction of *Mtk* expression by forced *GBP* expression was measured in larvae whose *Pvr* expression was significantly repressed as shown in Supplementary Fig. 8. Each value represents the mean \pm s.d. for five independent determinations. ** $P < 0.01$: Significant differences from control (*UAS-dsPvr*;*UAS-GBP*) value are indicated by Tukey's HSD.

GBP-mediated immunopolarization in single cells. Finally, we used transgenic *Drosophila* larvae expressing green fluorescence protein (GFP) under the control of the *Mtk* promoter. When we isolated plasmatocytes from the transgenic larvae injected with GBP, we found that the fluorescent signal was not uniformly distributed (Fig. 6a). Most of the strong fluorescent signals were found in the rounded (non-spread) plasmatocytes, but little or no signal was observed in spread cells (Fig. 6a–c; Supplementary Fig. 9). These data strongly indicated that, in the presence of GBP, a single plasmatocyte cannot simultaneously exert both arms of the immune response. We used the same reporter assay for the *Mtk* promoter in S2 cells (Fig. 6d). One hour after GBP treatment, we observed that the GFP signal was lost during the transition from non-spread to spread cells (Fig. 6d). We further conclude that, through its actions on individual cells, GBP enhances one arm of the immune pathway—either the humoral or cellular response—while inhibiting the other (Fig. 6e). We can describe this phenomenon as immunophysiological polarization. It is initiated by GBP in cooperation with the Pvf/Pvr signalling cascade. This represents a new development in our understanding of

the molecular basis by which insects mount a defense against invading pathogens.

Discussion

Our study breaks new ground by demonstrating reciprocal coordination of the humoral and cellular arms of an innate immune program in insect plasmatocytes and *Drosophila* S2 cells. Furthermore, we provide a molecular characterization of the signalling cascades that are responsible for this immunophysiological polarization. For example, we used the *Drosophila* S2 cell line to characterize a linear, multistep pathway by which GBP promotes cell spreading, a phenomenon that is generally regarded as the initiation of the cellular immune response. This work includes demonstrating a novel role in immunity for the PLC signalling system. We have further shown that the autocrine Pvf/Pvr loop is one of the signalling events that is activated downstream of GBP. This is not only a previously unknown function for GBP, but is also a finding that counters previous proposals that the Pvf/Pvr pathway is a general inhibitor of

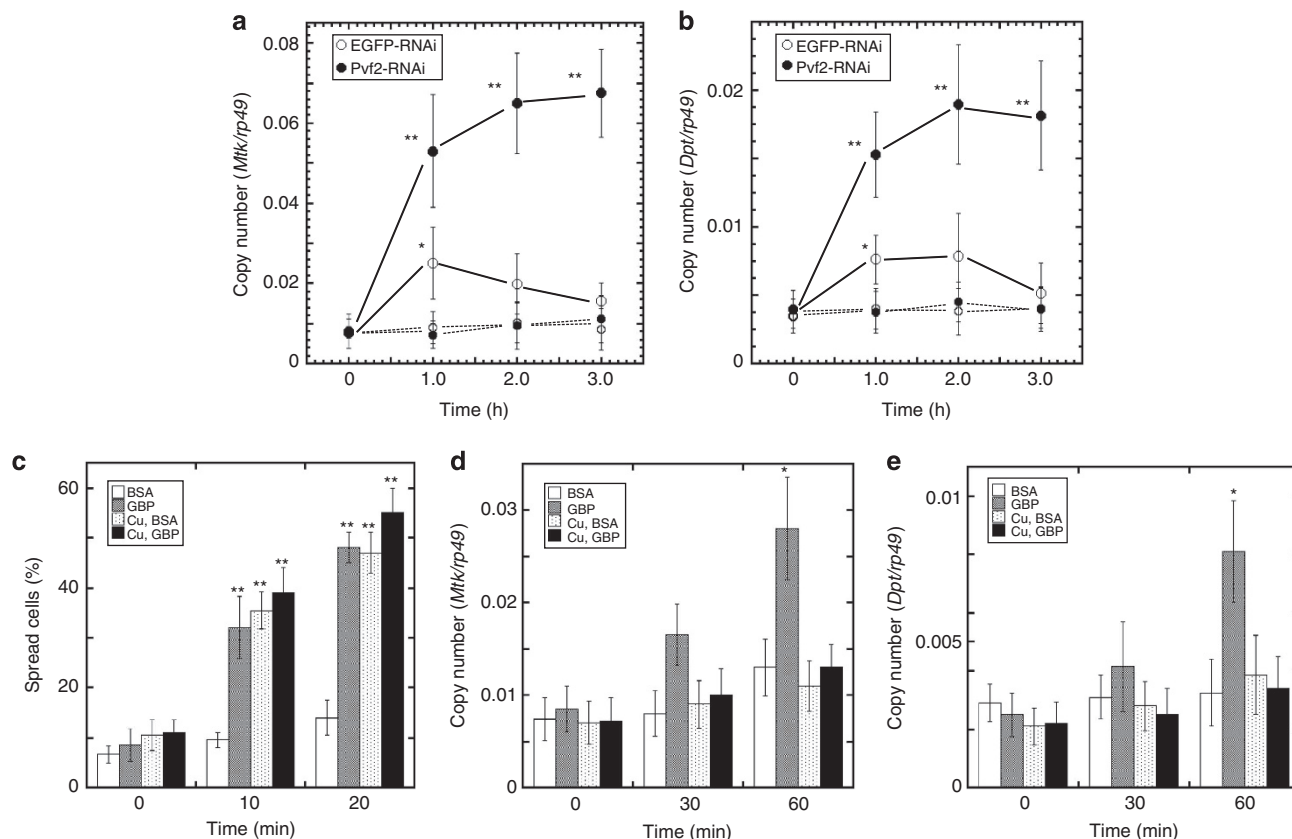


Figure 5 | Effects of Pvf/Pvr signalling on cellular and humoral immune responses of *Drosophila* S2 cells. (a) Effect of dsRNA targeting of *Pvf2* on GBP-induced *Mtk* expression. Fifty nM GBP was added into each well containing 1×10^6 S2 cells. Control values without GBP were shown by dotted lines. Each value represents the mean \pm s.d. for five independent determinations. * $P < 0.05$; ** $P < 0.01$: Significant differences from control (0 min) value are indicated by Tukey's HSD. **(b)** Effect of dsRNA targeting of *Pvf2* on GBP-induced *Dpt* expression. Other explanations are as in **a**. **(c)** Effect of *Pvf2* overexpression on GBP-induced S2 cell spreading. *Pvf2* expression was induced by addition of CuSO_4 into the culture medium. Fifty nM GBP or BSA was added to S2 cells for the indicated times. Each value represents the mean \pm s.d. for five independent determinations. ** $P < 0.01$: Significant differences from control (0 min, BSA) value are indicated by Tukey's HSD. **(d)** Effect of *Pvf2* overexpression on GBP-induced *Mtk* expression in S2 cells measured as described in **(a)**. Each value represents the mean \pm s.d. for five independent determinations. * $P < 0.05$: Significant difference from control (0 min, BSA) value is indicated by Tukey's HSD. Other explanations are as in **c**. **(e)** Effect of *Pvf2* overexpression on GBP-induced *Dpt* expression in S2 cells measured as described in **b**. Other explanations are as in **d**.

immune responses^{18,32}. We have now demonstrated that the Pvf/Pvr pathway serves a more complex, coordinating role than was previously appreciated; its activation downstream of GBP downregulates humoral immune responses in favour of initiating a cellular-based immunity program—all in the same cells. Our characterization of GBP as a pivotal regulator of the nature of an insect's response to invading pathogens could be pertinent to human health, since the mechanisms and principles of innate immunity are so highly conserved.

The success of our study owes much to the S2 hemocyte-like cell line being a convenient, yet powerful model for studying immune responses in *Drosophila*^{16,18}. While plasmatocytes can be obtained from *Drosophila* larvae, the isolation procedures are tedious and the yields are low. We have now added to the value of S2 cells in immunity research by demonstrating that GBP promotes spreading of these cells (Fig. 1), an initial step in the acquisition of an encapsulating phenotype. The GBP provides a convenient means of determining physiological response to specific signalling activities, such as the PLC/ Ca^{2+} cascade^{16,23}. It was also the genetic tractability of S2 cells that allowed us to determine that *Pvf* knockdown strongly inhibited GBP-dependent cell spreading while upregulating expression of the humoral effector gene, *Mtk*. That is, the S2 cells exhibited immunopolarization. While observations made with S2 cells might not

always recapitulate immunological phenomena that take place *in vivo*, we also observed immunopolarization in individual plasmatocytes that were obtained from *Drosophila* larvae treated with RNAi against *Pvr*: these cells exhibited enhanced expression of *Mtk* but impaired cell spreading (Figs 4 and 5). Similar to an earlier study⁸, we found that overexpression of GBP *in vivo* slightly stimulated *Mtk* expression, but to a level that was ~ 10 -fold less than that induced on bacterial infection (Fig. 4d). Previously, the significance of that observation was unclear⁸. Our current study has now clarified that the relatively weak effect of GBP overexpression in *Drosophila* larvae reflects a role of *Pvr* in downregulating humoral immune responses¹⁸ (Fig. 4d). Our elucidation of these 'gatekeeper' roles for the Pvf/Pvr loop suggest that it may be profitable for future research to investigate whether regulation of the expression of these particular genes influences polarization of plasmatocytes between cellular and humoral phenotypes, for example, in response to the degree of the pathogenic challenge, or in response to microenvironmental fluctuations.

One intriguing observation is that a few minutes treatment with the protease inhibitor APMSF led to inhibition of GBP-dependent activation of ERK via the Pvf2/Pvr signalling pathway (Fig. 2e). In such experiments, APMSF is not expected to enter cells^{33,34}. Furthermore, APMSF does not affect GBP-mediated

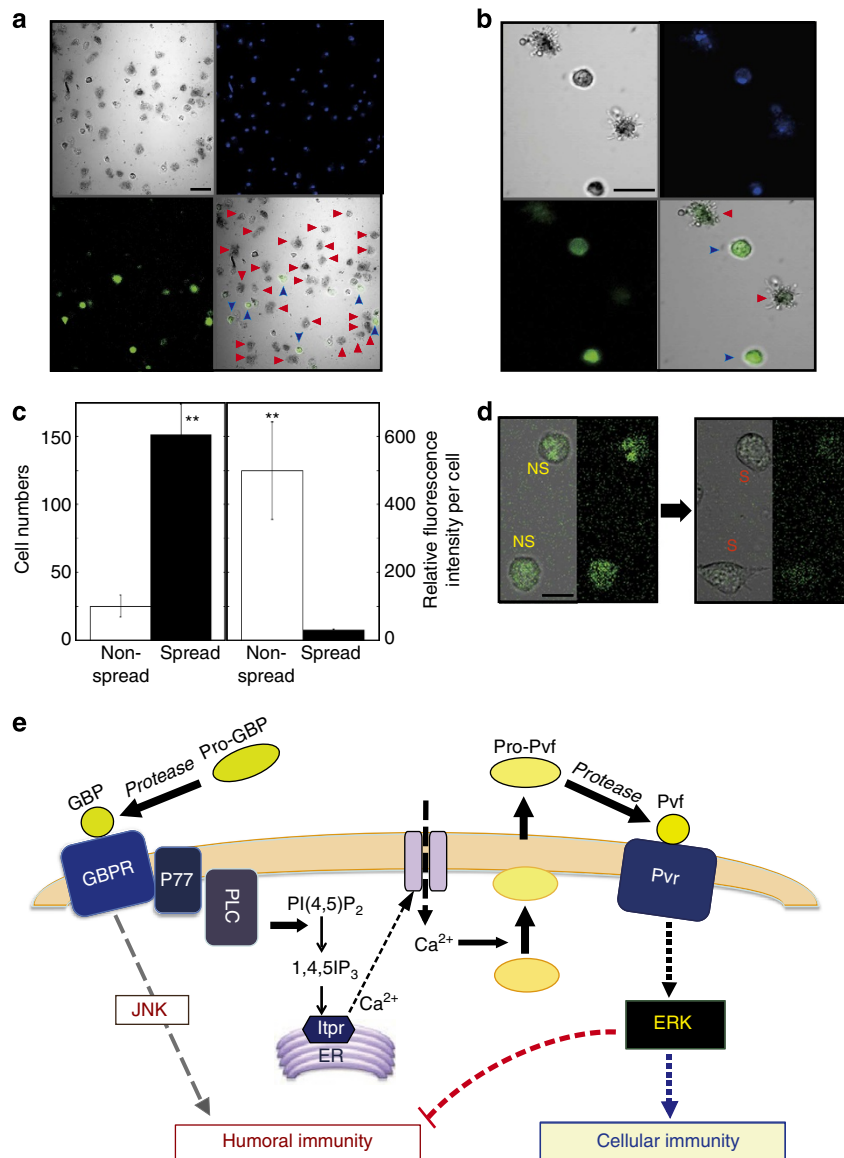


Figure 6 | GBP effect on a reporter assay for *Metchnikowin* expression in *Drosophila* plasmatocytes and S2 cells, and a model of the GBP signalling pathway. (a) Low magnification view of *Drosophila* plasmatocytes. Larvae expressing GFP under the control of the *Mtk* promoter were injected with ~20 nmol per larva of GBP, 1 h before plasmatocytes were prepared. Non-spread (blue arrowhead) and spread (red arrowhead) plasmatocytes were observed by laser scanning confocal microscopy (EZ-Ti, Nikon). Scale bar, 20 μ m. (b) High magnification view of *Drosophila* plasmatocytes. Other explanations are as in a. (c) Quantitative analysis of GFP expression in non-spread and spread cells. Cell morphology was scored by counting ~200 cells from a randomly selected view. Average fluorescent signal intensities of each cell were quantified by the confocal microscope software EZ-C1 (Nikon). Each value represents the mean \pm s.d. for four independent determinations ($P < 0.01$): Significant differences are indicated by Tukey's HSD. (d) Effect of GBP on GFP expression in S2 cells expressing GFP under the control of the *Mtk* promoter. One hour after addition of 50 nM GBP, S2 cells were analysed by confocal microscopy as described in a. Scale bar, 10 μ m. (e) Overview of the new positive and negative regulatory features of the GBP signalling pathway described in the current study: Stimulation of PLC by activated GBPR produces IP_3 , which promotes extracellular Ca^{2+} influx. We have previously demonstrated the presence of GBPR together with its adaptor protein (P77) ref. 38,42. Elevated Ca^{2+} triggers secretion of Pvf which stimulates Pvr. Activation of Pvr in turn promotes ERK phosphorylation, which activates cellular immune responses (cellular immunity) such as encapsulation while simultaneously repressing the expression of immune effector molecules such as *Mtk* (humoral immunity). See the text for discussion of the possibility that Pvf2 may be activated by proteolysis.**

Ca^{2+} mobilization (Fig. 2c). We therefore speculate that Pvf2 may require proteolytic processing to be activated; that is a process that could account for sensitivity to APMSF. However, further experiments are required to investigate that possibility.

It is known that innate immune responses exhibit a high degree of evolutionary conservation. For example, the platelet-derived growth factor receptor is a mammalian homologue of *Drosophila* Pvr²⁹. Moreover, professional phagocytes in mammals—such as

macrophages—undergo immunophysiological polarization³⁵. This can manifest itself as a balance between competing pro- and anti-inflammatory phenotypes, and there are also instances where cellular and humoral responses are differentially regulated. The degree of polarization reflects both the nature of the threat to the host, and changes in microenvironmental conditions; the signalling mechanisms that underlie these complex responses are poorly understood³⁶. Thus, the possibility that there may be a

human homologue of GBP and conservation of its mechanisms of action, are both subjects that deserve further investigation.

It is well recognized that innate immunity in insects involves both humoral and cellular defense strategies. These two processes are often viewed as being cooperative and functionally equivalent^{3,11}. However, in recent years, a competing viewpoint has emerged that depicts cellular activities such as phagocytosis and encapsulation as being somewhat independent 'first responders'^{9,37}. This hypothesis further depicts the induction of humoral responses, such as the transcription of *AMP* gene products, as a secondary, delayed response^{9,37}. Our study provides strong new support for the latter ideas. Moreover, we show that the delay before humoral genes are induced need not be passive; that is another key conclusion to emerge from our study, which demonstrates that GBP actively restrains humoral response processes through the Pvf/Pvr signalling pathway. Further studies aimed at revealing the regulatory mechanism of Pvf/Pvr signalling activities in immune cells should enhance understanding of the overall regulation of GBP-induced immunophysiological polarization in insects.

Some beneficial outcomes of this measured, GBP-dependent sequential defense strategy may be proposed. First, it is strikingly efficient to deploy a single upstream mediator—GBP—rather than a range of cross-regulatory agonists, to reciprocally regulate two different physiological responses. Second, limiting the role of the humoral defenses may minimize the negative consequences of antagonistic pleiotropy: humoral immune genes have other functions in growth and development, and so organismal homeostasis may be less perturbed while the insect attempts to first neutralize an invading pathogen by phagocytosis and encapsulation. Third, since heightened immunity has a negative impact on other life traits, a calibrated immune response may more efficiently manage the investment in resources that are required to fight infection. Our conclusion that GBP can enforce the timing of the induction of these different components of the overall immune response reveals the importance of this peptide in managing survival of the organism with minimal cost to its overall fitness.

Methods

Animals and Cells. *P. separata* larvae were reared on an artificial diet (10% kidney beans, 10% wheat bran, 4.2% dried yeast, 0.5% ascorbic acid, 0.3% antiseptic reagents and 1.3% agar) at 25 °C with a photoperiod of 16 h light: 8 h dark³⁸. *Drosophila melanogaster* stocks were reared on cornmeal–glucose–yeast medium at 23 °C³⁹. The *UAS-dsPvr* strains were supplied by NIG-FLY (National Institute of Genetics). The *Mtk-GFP* strain was gift from Jean-Luc Imler (Institut de Biologie Moléculaire et Cellulaire, Strasbourg, France)⁴⁰. We generated *Pvr* knockdown and GBP overexpressed transgenic flies controlled by the *hs-Gal4* driver^{8,41}.

Drosophila S2 cells were maintained Schneider's *Drosophila* medium (Gibco, USA) was supplemented with 5% fetal bovine serum (FBS), 50 units ml⁻¹ penicillin and 50 µg ml⁻¹ streptomycin at 25 °C.

Peptides. *P. separata* GBP (ENFSGGCVAGYMRTPDGRCKPTF), *D. melanogaster* GBP (ILLETTQKCKPGFELFGKRCRKA) and Pvf2 peptide fragment (CPRPGLPNRNPNLQRLQSKRQNGKS) were synthesized and purified by reversed-phase C₈ HPLC column (5-µm particle size, 4.6 × 250 mm, pore size = 300 Å; YMC, Japan)⁴².

Cell-Spreading Assay. *P. separata* haemolymph was collected into an ice-cold microcentrifuge tube containing 1 ml of anticoagulant buffer (41 mM citric acid, 98 mM NaOH, 186 mM NaCl, 1.7 mM EDTA, pH 4.5) and immediately centrifuged at 500g for 1 min at 4 °C. Precipitated hemocytes were suspended in 1 ml anticoagulant buffer and, after leaving on ice for 30 min, cells were used for preparation of plasmatocytes. For isolation of plasmatocytes (over 90% purity), Percoll step-gradient centrifugation was used according to the method of Clark *et al.*¹² Whole isolated plasmatocytes were washed twice with anticoagulant buffer and once with Ex-Cell 420 medium (JHR Bioscience, Hampshire, UK) by repeating suspending and centrifugation at 500g. Washed cells were finally resuspended in Ex-Cell 420 medium (2 × 10⁴ cells ml⁻¹) containing GBP at 25 °C. The percentage of plasmatocytes spread in an assay was scored 20–30 min after mixing cells and

peptide by counting 100 cells from a randomly selected view. The proportion of flattened and spread plasmatocytes was then recorded. *Drosophila* larval hemocytes were collected into an ice-cold microcentrifuge tube containing 100 µl of anticoagulant buffer and immediately centrifuged at 500g for 2 min at 4 °C. Precipitated hemocytes were suspended in Schneider's *Drosophila* medium (1 × 10⁴ cells ml⁻¹) and directly used for spreading assay, because it is known that most of the larval hemocytes (over 90%) are plasmatocytes in healthy larvae. S2 cells were collected from a stock culture flask 2–3 days after seeding, and washed twice with Schneider's *Drosophila* medium. Washed cells were suspended in 500 µl same medium (1 × 10⁵ cells ml⁻¹) and, after leaving on ice for 60 min, cells were used for spreading assays. The degree to which the normally spherical plasmatocytes (or S2 cells) adopted a more flattened, spread phenotype was assessed by micrometric analysis. Cells were regarded as spread when they became flattened when their longest axis ≥ 35 µm (for *P. separata* plasmatocytes), ≥ 24 µm (for *D. melanogaster* plasmatocytes) and ≥ 25 µm for (S2 cells).

Quantitative RT-PCR Analysis. To quantify *Drosophila* gene expression in *Drosophila* S2 cells or larval hemocytes, RT-PCR was conducted essentially according to the previously described procedure as follows²⁴. Total RNAs of S2 cells or *Drosophila* hemocytes were prepared from larvae injected with ~20 nmol per larva GBP or BSA 60 min after the injection. First-strand cDNA was synthesized with oligo(dT)_{12–18} primer using ReverTra Ace RT-PCR kit (Toyobo, Japan) according to the manufacturer's protocol. The cDNAs for target genes were amplified with a specific primer pair indicated in Supplementary Table 1. PCR was conducted under the following conditions: 20–28 cycles at 95 °C for 30 s, 58 °C for 30 s, and 72 °C for 45 s. Quantitative real-time PCR was carried out with the cDNAs in a 20 µl reaction volume of LightCycler Fast DNA Master SYBR Green I (Roche Applied Science, USA), using the Light-Cycler 1.2 instrument and software (Roche Applied Science). The PCR cycling conditions were denaturation at 95 °C for 10 min, followed by 45 cycles of 95 °C for 10 s, annealing at 55 °C for 5 s and extension at 72 °C for 15 s. Using the second derivative maximum method provided in the LightCycler software (version 3.5), a standard curve was generated by plotting the external standard concentration against threshold cycle. The software automatically calculated PCR product concentration for each tissue sample. All samples were analysed in duplicate, and assay variation was typically within 10%. Data were normalized according to the expression level of *rp49* determined in duplicate by reference to a serial dilution calibration curve. All primers used in this study were listed in Supplementary Table 1.

Measurements of inositol phosphates. All experiments were performed at 25 °C. S2 cells (6-well dish; each well contained 5 × 10⁵ cells in 2 ml) were labelled for 4 days with [³H]myo-inositol (Perkin Elmer; 35 µCi per ml). After 2 days, fresh media and [³H]myo-inositol were added. On day 4, the medium was replaced with a serum-free medium (either Schneider's *Drosophila* medium or HEPES-buffered salt solution (120 mM NaCl, 20 mM HEPES (pH 7.4 with NaOH), 5.4 mM KCl, 0.8 mM MgCl₂, 10 mM glucose, and unless otherwise stated, 1 mM CaCl₂). After a further 1–3 h, LiCl was added to a final concentration of 10 mM for 20 min and then *Drosophila* GBP was added for various times. Assays were quenched by aspiration of media followed immediately by the addition of 1 ml ice-cold 0.6 M perchloric acid per 0.02 mM InsP₆. After 20 min on ice, soluble material was removed and neutralized with 0.4 ml of 1 M potassium bicarbonate/0.04 M EDTA. Samples were stored at 4 °C overnight, centrifuged to remove insoluble potassium perchlorate, diluted 1:1 with 1 mM EDTA and then analysed either by a Q-100 HPLC (4.6 × 250 mm; Thomson Instruments, USA) with an in-line detector²³.

Double-stranded RNA-mediated interference *in vitro*. Individual DNA fragments ~700 bp in length, containing coding sequences for the proteins to be 'knocked down' were amplified by using PCR. Each primer used in the PCR contained a 5' T7 RNA polymerase binding site (5'-GAATTAATACGACTC ACTATAGGGAGA-3') followed by sequences specific for the targeted genes (see Supplementary Table 1). The PCR products were purified and were used as templates by using a Megascript T7 transcription Kit (Ambion, USA) to produce dsRNA according to the manufacturer's protocol. Ten micrograms of dsRNA were analysed by 1.5% agarose gel electrophoresis to ensure that the majority of the dsRNA existed as a single band of ~700 bp. S2 cells were incubated at 1 × 10⁵ cells per well in 96-well plate in 1 × Schneider's *Drosophila* media with 5% FBS at 25 °C. dsRNA was added directly to the media to a final concentration of 37 nM. The cells were incubated for three days to allow for turnover of the target protein.

Expression of Pvf2 or Mtk-GFP in *Drosophila* S2 cells. Overexpression of *Pvf2* in *Drosophila* S2 cells were performed using pCoHygro vector (Invitrogen) according to procedure of Kellenberger *et al.*⁴³ Cells were used 3–4 days following induction of *Pvf2* by addition of 0.5 mM CuSO₄. S2 cells were used for a series of assays. The *Mtk-GFP* construct (1,495 bp of *Mtk* upstream sequences fused with the jellyfish *Aequorea victoria GFP*)⁴⁰ was cloned into the pMT-V5 His vector and co-transfected into S2 cells with pCoHygro vector. S2 cells were propagated in 1 × Schneider's *Drosophila* medium with 5% FBS at 25 °C.

Analysis of ERK phosphorylation. S2 cells were collected into an ice-cold microcentrifuge tube containing 1 ml of anticoagulant buffer and immediately washed twice with anticoagulant buffer. Washed cells were solubilized by adding same volume of $2 \times$ lysis buffer (100 mM HEPES-NaOH, 300 mM NaCl, 3 mM MgCl₂, 1 mM EDTA, 20% glycerol, 2% TX-100 (w/v), 1% sodium deoxycholate, 0.2% SDS, pH 7.5) containing Protease inhibitor cocktail (Nacalai tesque, Japan), phosphatase inhibitor cocktail set II (Calbiochem, USA), and 0.2% phenylthiourea. After centrifugation at 17,000 g for 15 min at 4 °C, the supernatant was mixed with the same volume of sample buffer (125 mM Tris-HCl, 10% 2-mercaptoethanol, 4% SDS, 10% sucrose, 0.004% bromophenol blue) and separated by SDS-PAGE (8 or 10%), transferred onto an Immobilon-P PVDF membrane (Millipore, USA). Proteins on the membrane were probed with anti-activated MAP Kinase (diphosphorylated ERK-1&2) mouse monoclonal antibodies (at 1:2,000, M9692, Sigma-Aldrich, USA)³⁸. For reprobing, membranes were washed for 30 min at 50 °C in 62.5 mM Tris-HCl (pH 6.7) containing 100 mM 2-mercaptoethanol and 2% SDS, and they were probed with anti-MAP kinase (ERK-1&2) mouse monoclonal antibodies (at 1:2,000, M5670, Sigma-Aldrich, USA). All positive bands were quantified using ImageJ (NIH).

Immunoblotting of Pvf2. The carboxy-terminal 26-amino-acid peptide of Pvf2 was coupled to keyhole limpet haemocyanin using the carbodiimide cross-linker, 1-ethyl-3-(3-dimethylaminopropyl)carbodiimide hydrochloride, emulsified in Titer Max Gold (CytRx, USA) and subcutaneously injected into a female rabbit to generate a specific polyclonal antibody. Anti-Pvf2 IgG was precipitated by adding ammonium sulphate to 40% saturation and further purified by an affinity column of protein G-Sepharose (GE Healthcare, USA). After collecting S2 culture medium, the medium was immediately mixed with -20 °C acetonitrile (final 30%) and centrifuged at 20,000g. for 10 min at 4 °C. The supernatant was concentrated by lyophilization, separated by SDS/PAGE and electrically transferred to a PVDF membrane filter. After blocking with BSA, polypeptides on the membrane were probed with anti-Pvf2 antibody (at 1:1,000)³⁸.

Measurements of Ca²⁺ response using GCaMP3-expressing *Drosophila* S2. S2 cell line that stably expresses GCaMP3 was established by co-transfection with pCoBlast and GCaMP3 harbouring pAc5.1/V5-HisA vectors using a Calcium Phosphate Transfection Kit basically according to the manufacturer's instruction (Invitrogen, USA). GCaMP3-expressing S2 cells were collected from a stock culture flask 3–4 days after seeding, and washed twice washed twice and incubated in Schneider's yeast-extract free and serum-free *Drosophila* medium (US Biological, USA). Approximately 1×10^5 cells per well were plated in 96-well plates and incubated for 1 h at 25 °C in 200 μ l medium, before the addition of indicated test samples. Calcium-induced fluorescence changes were recorded simultaneously in all wells using a FLIPR-TETRA (Molecular Devices).

Analysis of GFP expression in plasmatocytes and *Drosophila* S2 cells. Whole haemolymph was collected from *Drosophila* larvae expressing *Mtk-GFP* into a 20 μ l drop of chilled Schneider's *Drosophila* medium (Invitrogen) 1 h after injection of $\sim 0.10 \mu$ l of 200 mM GBP. Soon after collecting haemolymph from 10 larvae, hemocytes were sedimented by centrifugation at 4 °C for 2 min at 500 g and suspended in Schneider's *Drosophila* medium. After nuclear staining with Hoechst 33258, fluorescence of GFP in hemocytes was monitored by laser scanning confocal microscope (EZ-Ti system, Nikon) using a 488-nm excitation filter in combination with a 515-nm emission filter. S2 cells were also observed in the same way by the confocal microscope. To quantify fluorescent intensities in each cell, we analysed approximately 200 cells from a randomly selected view and identified as non-spread and spread cells by micrometric analysis. We next measured fluorescent intensities in these cells by the confocal software EZ-C1 (Nikon) and these values were divided by the cell areas. We performed this analysis for control and GBP-treated cells.

Infection and injury experiments. Direct bacterial infection experiments was induced by stabbing third instar larvae with a thin tungsten needle (diameter: ~ 0.05 mm) previously dipped into a concentrated culture of *Serratia marcescens* ($OD_{600} = 1 \times 10^{-2}$).

Statistics. Statistical significance was examined by analysis of variance with a Tukey's HSD *post hoc* test.

References

- Lemaitre, B. & Hoffmann, J. The host defense of *Drosophila melanogaster*. *Annu. Rev. Immunol.* **25**, 697–743 (2007).
- Strand, M. R. The insect cellular immune response. *Insect Sci.* **15**, 1–14 (2008).
- Tsakas, T. & Marmaras, V. J. Insect immunity and its signalling: an overview. *Invertebrate Survival Journal* **7**, 228–238 (2010).
- Kounatidis, I. & Ligoxygakis, P. *Drosophila* as a model system to unravel the layers of innate immunity to infection. *Open Biol.* **2**, 120075 (2012).
- Lanot, R., Zachary, D., Holder, F. & Meister, M. Postembryonic hematopoiesis in *Drosophila*. *Dev. Biol.* **230**, 243–257 (2001).
- Wood, W. & Jacinto, A. *Drosophila melanogaster* embryonic haemocytes: masters of multitasking. *Nat. Rev. Mol. Cell Biol.* **8**, 542–551 (2007).
- Koppen, T. *et al.* Proteomics analyses of microvesicles released by *Drosophila* Kc167 and S2 cells. *Proteomics* **11**, 4397–4410 (2011).
- Tsuzuki, S. *et al.* *Drosophila* growth-blocking peptide-like factor mediates acute immune reactions during infectious and non-infectious stress. *Sci. Rep.* **2**, 210 (2012).
- Ye, Y. H., Chenoweth, S. F. & McGraw, E. A. Effective but costly, evolved mechanisms of defense against a virulent opportunistic pathogen in *Drosophila melanogaster*. *PLoS Pathog.* **5**, e1000385 (2009).
- Aggarwal, A. & Silverman, N. Positive and negative regulation of the *Drosophila* immune response. *BMB Rep.* **41**, 267–277 (2008).
- Lavine, M. D. & Strand, M. R. Haemocytes from *Pseudoplusia includens* express multiple alpha and beta integrin subunits. *Insect Mol. Biol.* **12**, 441–452 (2003).
- Clark, K. D., Pech, L. L. & Strand, M. R. Isolation and identification of a plasmatocyte-spreading peptide from the hemolymph of the lepidopteran insect *Pseudoplusia includens*. *J. Biol. Chem.* **272**, 23440–23447 (1997).
- Matsumoto, H., Tsuzuki, S., Date-Ito, A., Ohnishi, A. & Hayakawa, Y. Characteristics common to a cytokine family spanning five orders of insects. *Insect Biochem. Mol. Biol.* **42**, 446–454 (2012).
- Strand, M. R., Hayakawa, Y. & Clark, K. D. Plasmatocyte spreading peptide (PSP1) and growth blocking peptide (GBP) are multifunctional homologs. *J. Insect Physiol.* **46**, 817–824 (2000).
- Abrams, J. M., Lux, A., Steller, H. & Krieger, M. Macrophages in *Drosophila* embryos and L2 cells exhibit scavenger receptor-mediated endocytosis. *Proc. Natl Acad. Sci. USA.* **89**, 10375–10379 (1992).
- Ramet, M. *et al.* *Drosophila* scavenger receptor CI is a pattern recognition receptor for bacteria. *Immunity* **15**, 1027–1038 (2001).
- Stuart, L. M. *et al.* A systems biology analysis of the *Drosophila* phagosome. *Nature* **445**, 95–101 (2007).
- Bond, D. & Foley, E. A quantitative RNAi screen for JNK modifiers identifies Pvr as a novel regulator of *Drosophila* immune signaling. *PLoS Pathog.* **5**, e1000655 (2009).
- Hayakawa, Y. Juvenile hormone esterase activity repressive factor in the plasma of parasitized insect larvae. *J. Biol. Chem.* **265**, 10813–10816 (1990).
- Hayakawa, Y. Structure of a growth-blocking peptide present in parasitized insect hemolymph. *J. Biol. Chem.* **266**, 7981–7984 (1991).
- Hayakawa, Y. Growth-blocking peptide: an insect biogenic peptide that prevents the onset of metamorphosis. *J. Insect Physiol.* **41**, 1–6 (1995).
- Srikanth, K., Park, J., Stanley, D. W. & Kim, Y. Plasmatocyte-spreading peptide influences hemocyte behavior via eicosanoids. *Arch. Insect Biochem. Physiol.* **78**, 145–160 (2011).
- Zhou, Y. *et al.* Activation of PLC by an endogenous cytokine (GBP) in *Drosophila* S3 cells and its application as a model for studying inositol phosphate signalling through ITPKI. *Biochem. J.* **448**, 273–283 (2012).
- Ninomiya, Y., Kurakake, M., Oda, Y., Tsuzuki, S. & Hayakawa, Y. Insect cytokine growth-blocking peptide signaling cascades regulate two separate groups of target genes. *FEBS J.* **275**, 894–902 (2008).
- Berridge, M. J. Inositol trisphosphate and calcium signalling mechanisms. *Biochim. Biophys. Acta* **1793**, 933–940 (2009).
- Watson, P. J., Fairall, L., Santos, G. M. & Schwabe, J. W. Structure of HDAC3 bound to co-repressor and inositol tetrakisphosphate. *Nature* **481**, 335–340 (2012).
- Agell, N., Bachs, O., Rocamora, N. & Villalonga, P. Modulation of the Ras/Raf/MEK/ERK pathway by Ca(2+), and calmodulin. *Cell. Signal.* **14**, 649–654 (2002).
- Schmitt, J. M., Wayman, G. A., Nozaki, N. & Soderling, T. R. Calcium activation of ERK mediated by calmodulin kinase I. *J. Biol. Chem.* **279**, 24064–24072 (2004).
- Duchek, P., Somogyi, K., Jekely, G., Beccari, S. & Rørth, P. Guidance of cell migration by the *Drosophila* PDGF/VEGF receptor. *Cell* **107**, 17–26 (2001).
- Zettervall, C. J. *et al.* A directed screen for genes involved in *Drosophila* blood cell activation. *Proc. Natl Acad. Sci. USA.* **101**, 14192–14197 (2004).
- Sims, D., Duchek, P. & Baum, B. PDGF/VEGF signaling controls cell size in *Drosophila*. *Genome Biol.* **10**, R20 (2009).
- Ragab, A. *et al.* *Drosophila* Ras/MAPK signalling regulates innate immune responses in immune and intestinal stem cells. *EMBO J.* **30**, 1123–1136 (2011).
- Okada, T. *et al.* A serine protease inhibitor prevents endoplasmic reticulum stress-induced cleavage but not transport of the membrane-bound transcription factor ATF6. *J. Biol. Chem.* **278**, 31024–31032 (2003).
- Wojcikiewicz, R. J. & Oberdorf, J. A. Degradation of inositol 1,4,5-trisphosphate receptors during cell stimulation is a specific process mediated by cysteine protease activity. *J. Biol. Chem.* **271**, 16652–16655 (1996).

35. Gratchev, A. *et al.* Mphi1 and Mphi2 can be re-polarized by Th2 or Th1 cytokines, respectively, and respond to exogenous danger signals. *Immunobiology* **211**, 473–486 (2006).
36. Liu, G. & Yang, H. Modulation of macrophage activation and programming in immunity. *J. Cell. Physiol* **228**, 502–512 (2012).
37. Haine, E. R., Moret, Y., Siva-Jothy, M. T. & Rolff, J. Antimicrobial defense and persistent infection in insects. *Science* **322**, 1257–1259 (2008).
38. Oda, Y. *et al.* Adaptor protein is essential for insect cytokine signaling in hemocytes. *Proc. Natl Acad. Sci. USA*. **107**, 15862–15867 (2010).
39. Ryuda, M. *et al.* Identification of a novel gene, anorexia, regulating feeding activity via insulin signaling in *Drosophila melanogaster*. *J. Biol. Chem.* **286**, 38417–38426 (2011).
40. Levashina, E. A., Ohresser, S., Lemaitre, B. & Imler, J.-L. Two distinct pathways can control expression of the gene encoding the *Drosophila* antimicrobial peptide Metchnikowin. *J. Mol. Biol.* **278**, 515–527 (1998).
41. Pili-Floury, S. *et al.* In vivo RNA interference analysis reveals an unexpected role for GGBP1 in the defense against Gram-positive bacterial infection in *Drosophila* adults. *J. Biol. Chem.* **279**, 12848–12853 (2004).
42. Ohnishi, A., Oda, Y. & Hayakawa, Y. Characterization of receptors of insect cytokine, growth-blocking peptide, in human keratinocyte and insect Sf9 cells. *J. Biol. Chem.* **276**, 37974–37979 (2001).
43. Kellenberger, C. *et al.* Structure-function analysis of grass clip serine protease involved in *Drosophila* Toll pathway activation. *J. Biol. Chem.* **286**, 12300–12307 (2011).

Acknowledgements

We thank the Bloomington Indiana Stock Center for supplying some of the basic stocks for this study. We thank John Patrenka for assistance with the calcium assays. This work was supported by a grant-in-aid for Scientific Research on Priority Areas from the Ministry of Education, Culture, Sports, Science and Technology of Japan, and also by the Intramural Research Program of the NIH/National Institute of Environmental Health Sciences.

Author contributions

S.T., H.M. and Y.H. carried out most experiments, S.F., M.R. and H.T. performed morphological experiments and analysis, E.J.S., G.S.B. and Y.Z. measured concentrations of calcium ion and inositol phosphates, S.B.S. and Y.H. planned the study and wrote the manuscript.

Additional information

Supplementary Information accompanies this paper at <http://www.nature.com/naturecommunications>

Competing financial interests: The authors declare no competing financial interests.

Reprints and permission information is available online at <http://npg.nature.com/reprintsandpermissions/>

How to cite this article: Tsuzuki, S. *et al.* Switching between humoral and cellular immune responses in *Drosophila* is guided by the cytokine GBP. *Nat. Commun.* **5**:4628 doi: 10.1038/ncomms5628 (2014).